Published in final edited form as:
J Am Chem Soc. 2002 May 1; 124(17): 4857–4864.

Time-Resolved Resonance Raman Analysis of Chromophore Structural Changes in the Formation and Decay of Rhodopsin's BSI Intermediate

Duohai Pan, **Ziad Ganim**, **Judy E. Kim**, **Michiel A. Verhoeven**†, **Johan Lugtenburg**†, and **Richard A. Mathies***
Department of Chemistry, University of California, Berkeley, California 94720, and Leiden Institute of Chemistry, Leiden University, 2300 RA Leiden, The Netherlands

Abstract

Time-resolved resonance Raman microchip flow experiments are performed to obtain the vibrational spectrum of the chromophore in rhodopsin's BSI intermediate and to probe structural changes in the bathorhodopsin-to-BSI and BSI-to-lumirhodopsin transitions. Kinetic Raman spectra from 250 ns to 3 μs identify the key vibrational features of BSI. BSI exhibits relatively intense HOOP modes at 886 and 945 cm^{-1} that are assigned to $C_{14}H$ and $C_{11}H{=}C_{12}H$ A_u wags, respectively. This result suggests that in the bathorhodopsin-to-BSI transition the highly strained all-trans chromophore has relaxed in the C_{10}-$C_{11}{=}C_{12}$-C_{13} region, but is still distorted near C_{14}. The low frequency of the 11,12 A_u HOOP mode in BSI compared with that of lumirhodopsin and metarhodopsin I idicates weaker coupling between the 11H and 12H wags due to residual distortion of the BSI chromphore near $C_{11}{=}C_{12}$. The $C{=}NH^+$ stretching mode in BSI at 1653 cm^{-1} exhibits a normal deuteriation indused downshift of 23 cm^{-1} implying that there is no significant structural rearrangement of the Schiff base counterion region in the transition of bathorhodopsin to BSI. However, a dramatic Schiff base environment change occurs in the BSI-to-lumirhodipsin transition. because the 1638 cm^{-1} $C{=}NH^+$ stretching mode in lumirhodopsin is unussully low and shifts only 7cm^{-1} in D_2O, suggesting that it has essentially no H-bonding acceptor. With these data we can for the first time compare and discuss the room temperature resonance Raman vibrational structure of all the key intermediates in visual excitation.

Introduction

Visual transduction in vertebrates is triggered by photon absorption in the visual pigment rhodopsin. Rhodopsin is a seven α-helical G protein-coupled receptor composed of 348 amino acids and an 11-*cis* retinal chromophore bound to Lys^{296} by a protonated Schiff base linkage.[1] The primary event in vision, the 11-*cis*-to-all-trans isomerization of retinal, is complete within 200 fs, [2,3] has a quantum yield of 0.65, [4] and produces a photoproduct that stores 146 kJ/mol (60%) of the incident photon energy. The primary photointermediate called photorhodopsin[3,5] has been shown by time-resolved Raman to be a hot and conformationally distorted form of the trans chromophore.[6] Photorhodopsin relaxes to bathorhodopsin (Batho), which then converts at room temperature through the blue-shifted intermediate (BSI) lumirhodopsin (Lumi), and metarhodopsin I (Meta I) leading to the deprotonation of the retinal Schiff base in metarhodopsin II (Meta II) and receptor activation.[7]

†Leiden University.
*To whom correspondence should be addressed at the University of California. E-mail: rich@zinc.cchem.berkeley.edu.

Understanding the structure and dynamics of rhodopsin's photointermediates is the key to the molecular mechanism of receptor activation. Early resonance Raman as well as FTIR experiments[8-11] on Batho trapped at low temperature revealed unusually intense hydrogen out-of-plane (HOOP) wagging vibrations of the chromophore in the 850-920 cm^{-1} region due to the 10, 11, 12, and 14 hydrogens. These data indicated that the $C_{11}=C_{12}$ trans chromophore structure in Batho is conformationally distorted and structurally perturbed near the $C_{11}=C_{12}$ positions. This structural perturbation in Batho is probably related mechanistically to its red-shifted absorption spectrum and its surprisingly efficient energy storage, [9,12-14] which is thought to provide the driving force for protein activation.

Batho relaxes to a blue-shifted intermediate (BSI), which then decays irreversibly to Lumi.[15] Since BSI is entropically favored, and lies higher in enthalpy than Batho by about 12 kJ/mol,[15] it is difficult to study BSI by low-temperature trapping techniques. To date a number of absorption and FTIR as well as site-directed mutagenesis experiments have been performed on pigment analogues to explore the structure and interactions of the BSI chromophore and protein.[16-19] However, the characterization of the native chromophore structure of BSI has not yet been accomplished. We were thus interested in obtaining timeresolved resonance Raman spectra of BSI at physiologically relevant temperatures to investigate how the chromophore structure changes in the transition from Batho-to-BSI and BSI-to-Lumi. This work should help to reveal how the energy stored in the Batho chromophore is used to drive protein conformational change.

We recently developed a Raman microchip flow technique and showed that it could be used to obtain high-quality, timeresolved Raman spectra of the Lumi and Meta I intermediates at room temperature on the micro- to millisecond time scale.[20] This technique is based on the use of microfabricated flow channels together with a Raman microprobe to excite and detect the scattering. These transient Raman spectra indicated that the structural relaxation of the chromophore—protein complex in the Batho-to-Lumi transition drives the Schiff base group out of its hydrogen-bonded environment near Glu113, while in the Lumi to Meta I transition, a fully planar chromophore with a normal Schiff base environment but presumably a different hydrogen-bond acceptor is formed. These experiments further demonstrated that the time-resolved resonance Raman microchip flow technique provides a very useful and convenient tool for getting detailed structural information about short-lived transient intermediates at room temperature.

Here we have performed time-resolved resonance Raman microchip flow experiments with higher 250 ns time resolution to obtain vibrational spectra of the native BSI intermediate. Kinetic measurements as well as the Raman spectrum of BSI in D_2O buffer allow us to characterize the vibrational structure and structural changes upon formation of BSI from Batho as well as its decay. These data provide new information on how the unique highly energetic conformational and structural perturbations of the chromophore in Batho relax as visual transduction proceeds.

Experimental Section

Preparation of Rhodopsin and Pigment Regeneration. Rhodopsin was isolated from 100 bovine retinas (J. A. Lawson, Lincoln, NE) by sucrose flotation followed by sucrose density gradient centrifugation as described previously.[9] The yield was typically 12-15 nmol of rhodopsin per retina. The isolated rod outer segments (ROS) were lysed in water and solubilized in 15 mL of 5% Ammonyx-LO (Exciton, dayton, OH). The resulting rhodopsin solution was further purified by hydroxylapatite column chromatography.[21] The final samples (150 mM phosphate buffer, pH 7, 7-11 mM NH_2OH) had an absorbance of 2.0- 2.5 OD/cm at 500 nm and 280/500 nm ratios of 1.76-1.90.

To prepare rhodopsin regenerated with isotopic retinal derivatives, ROS are first bleached by ambient light in the presence of 20 mM hydroxylamine. The bleached sample is pelleted and washed with phosphate buffer three times to remove excess hydroxylamine and retinal. The regeneration is performed by adding a 1.5-fold molar excess of 14d-11-*cis* retinal and incubating for approximately 15 h at room temperature until no additional growth is observed in the absorption at 500 nm. The regenerated sample is solubilized in Ammonyx-LO detergent and purified as described above.

Transient Resonance Raman Spectroscopy. Transient resonance Raman spectra were obtained by using a time-resolved Raman microchip apparatus as described previously (Figure 1).[20] Briefly, a beam splitter (50/50) was first used to make the probe and pump beams nearly collinear. A 250 mm focal length cylindrical lens then focused the 531 nm pump beam and the 458 nm probe to the microprobe image plane. The line image of the beam was subsequently focused on the flowing sample by a 40 × NA 0.6 objective lens to form ~3 × 100 μm spots for both the probe and pump beams. Adjusting the beam splitter position with a translation stage gives the desired spatial separation between the two beams. The spatial separation was determined by measuring the center-to-center distance between the two beam image lines on the entrance slit of the spectrograph with a periscope viewer.

The microchips were fabricated from glass substrates using photolithography, wet chemical etching, and thermal bonding methods.[22,23] The advantage of this microfabricated system is that very small amounts of sample are needed because the flow cross section can be made very close to the imaged laser beam size. For example, only 10 mL of sample was needed for the pump-plus-probe spectrum and only 2 mL was required for the probe-only spectrum. The channel dimensions of the chip used in our experiments are ~ 42 μm deep × 142 μm wide.

The laser powers and flow rates were chosen to give the desired time delays and photoalteration parameters *F*.[24] BSI coexists with Batho in an equilibrium mixture and decays with a 290 ns lifetime at 5 °C.[15] To detect transient Raman scattering from BSI, the overlapping pump and probe beams are separated by ~ 0.7 μm, providing a delay time of ~250 ns (flow speed of 280 cm/s). The 531 nm pump (2.5 mW) and 458 nm probe (450 μW) were selected to produce photoalteration parameters of 3 for rhodopsin and 0.3 for BSI, respectively.

Backscattered Raman light was collected by the objective and focused on the entrance slit of the subtractive dispersion, double spectrograph.[25] Typically the optical density (Od) of the sample is around 2.0-2.5/cm at 500 nm giving an Od of ~0.01 in the channel. It was necessary to record ten ~1 min exposures for each experimental configuration. Cosmic ray spikes were removed from each spectrum before summation. Raman spectra were detected with a cooled backilluminated CCD detector (LN/CCD-1100/PB, Princeton Instruments) controlled by a ST-133 controller. All spectra were corrected for the wavelength dependence of the spectrometer efficiency by using a white lamp. The fluorescence background was removed by subtracting a bleached rhodopsin spectrum. The known cyclohexane Raman peaks were used to calibrate the spectra. The reported frequencies are accurate to ±2cm^{-1}, and the resolution of the spectra is 6 cm^{-1}.

Computational Methods. The structural model of rhodopsin and its intermediates was built using Insight II. The energy minimization was done with discover (Molecular Simulations, San diego). The intermediate structures were determined by modifying the 3-d X-ray structure[26] and incorporating experimentally determined[27,28] retinal backbone distances and protonated Schiff base to E113 distances. CD[29] and binding studies[30] with retinal analogues have argued for a negative C_{12}-C_{13} twist while theory[31] supports a positive twist angle. In the absence of a definitive conclusion, we have set the C_{12}-C_{13} twist angle in rhodopsin to be -140° and consistently employed negative twist angles for the other intermediates although additional

work on this question is clearly needed. In Batho, the twist angles of C_{10}-C_{11},C_{12}-C_{13}, and C_{14}-C_{15} were set to -20°, -20°, and -56°, respectively, based on Raman studies.[8] The distance (4.3 Å) between the carbon atom of E113 and the Schiff base proton in Batho was set to be the same as that in rhodopsin because they have nearly the same protonated Schiff base environment immediately after cis-trans isomerization.[32] In BSI, the retinal assumes a more relaxed conformation as indicated by significantly reduced HOOP mode intensities. We thus assumed significant relaxations of the C_{10}-C_{11} (-9°) and C_{12}-C_{13} (-10°) bonds. Because the new intense HOOP mode at 886 cm^{-1} in BSI is assigned to the $C_{14}H$ wag, the twist angle of C_{14}-C_{15} is only reduced to -46°. Raman intensities of the HOOP modes are somewhat weaker in Lumi so the twist angles of C_{10}-C_{11},C_{12}-C_{13}, and C_{14}-C_{15} were reduced to -4°, -2°, and -9°, respectively. The distances from the PSB proton to the carbon atom of E113 in BSI and Lumi are 3.8 and 4.0 Å, respectively. Since previous NMR and FTIR studies predicted that the interaction between the counterion and the Schiff base would be mediated by water molecules,[33,34] two water molecules were added near E113 and the Schiff base in rhodopsin, Batho, as well as BSI, which are not present in X-ray structure.[26]

Results

The photobleaching scheme of rhodopsin at room temperature is described as follows:

$$\mathrm{Rho} \xrightarrow{h\nu} \mathrm{Batho} \underset{k_1^{r}}{\overset{k_1^{f}}{\rightleftarrows}} \mathrm{BSI} \xrightarrow{k_2} \mathrm{Lumi} \xrightarrow{k_3} \mathrm{Meta}\ I$$

where k_1^f and k_1^r are 4.44×10^6 s^{-1}, k_2 is 3.4×10^6 s^{-1}, and k_3 is 1.0×10^5 s^{-1} at 5 °C.[15] This kinetic scheme was solved numerically to estimate the concentrations under our illumination conditions, and the results are presented in Figure 2. BSI has a relatively low concentration because it is in equilibrium with Batho. Therefore, the transient Raman spectra will consist of scattering from a mixture of Batho, BSI, and Lumi. Raman intensity is proportional to the concentration of each species times the relative Raman cross section. The latter quantity is roughly proportional to the square of the extinction coefficient. For BSI experiments, the probe excitation wavelength is selected to be 458 nm, which is distant from the Batho absorption band (λ_{max} = 531 nm). The contribution of Batho to the transient spectrum at 250 ns can thus be neglected. Assuming that the relative Raman cross sections of BSI and Lumi at 458 nm are the same,[15] one predicts that at 250 ns 58% of the scattering will come from Lumi and 42% from BSI. The BSI lifetime increases with decreasing temperature[15] so the samplereservoir was cooled with ice to ~1 °C to produce the highest possible concentration of BSI. When the sample was pumped through the microfabricated channel to the microprobe image plane, the temperature warmed to ~7 °C.

Figure 3 presents the results of time-resolved resonance Raman microchip flow experiments on the BSI intermediate. First, a probe-only Raman spectrum of rhodopsin was obtained using 458 nm excitation (Figure 3B). The pump-plus-probe spectrum with a 250 ns time delay in Figure 3A exhibits new bands at 886 and 947 cm^{-1}, suggesting it contains scattering from BSI. Subtraction of the probe-only spectrum (0.86) from the pump-plus-probe spectrum to minimize the positive or negative 971, 1238, and 1267 cm^{-1} intensities of rhodopsin gives a difference spectrum (Figure 3C). No HOOP bands at 853, 876, and 921 cm^{-1}, characteristic of the chromophore structure of Batho, could be identified in this Raman spectrum. The difference spectrum is thus dominated by scattering from the Lumi and BSI intermediates. To get a pure BSI Raman spectrum, we carried out a time-resolved resonance Raman experiment with a time delay of 3 μs and the same pump and probe configuration (spatial separation of 8 μm and flow speed of 250 cm/s), which yields a Lumi spectrum (Figure 3D). This spectrum was identical to our previously reported Lumi Raman spectrum.[20] The pure BSI spectrum was obtained by subtracting the Lumi spectrum from the transient Raman spectrum with a 250 ns time delay,

using the characteristic 1638 cm^{-1} Schiff base band of Lumi as a marker band for the Lumi contribution. Subtraction of the Lumi spectrum from this transient spectrum (factor 0.5) to minimize the 1638 cm^{-1} band yields a spectrum in the BSI intermediate (Figure 3E). The uncertainty in this subtraction parameter is ~8%; undersubtraction leaves a noticeable band at 1638 cm^{-1} due to Lumi while oversubtraction leaves a clear derivative feature.

Figure 4 presents transient Raman spectra of BSI and Lumi mixtures for time delays from 250 ns to 3 μs to explore the temporal dependence of the BSI features. The spectrum with a ~250 ns time delay (Figure 4A) is characterized by a new HOOP band at 886 cm^{-1} and two Schiff base lines at 1638 and 1653 cm^{-1}. It is clear from Figure 4 that the intensity of the lines at 886 cm^{-1} in the HOOP region and 1653 cm^{-1} in the Schiff base region are initially large, then drop appreciably in the 700 ns spectrum and disappear in the 3 μs spectrum, while the 1638 cm^{-1} band increases significantly from 250 ns to 3 μs. Furthermore, the 1552 cm^{-1} ethylenic band in the 250 ns spectrum downshifts to 1548 cm^{-1} in the 3 μs spectrum, implying that two different intermediates contribute to the spectra. Since the Lumi formation time is ~1 μs, the spectrum in Figure 4C is expected to be dominated by scattering from the Lumi intermediate. The spectrum in Figure 4C is also identical to the Lumi spectrum with a 16 μs time delay obtained by using probe and pump wavelengths of 514.5 and 488 nm, respectively.[20] As a result, the new HOOP band at 886 cm^{-1} and the 1653cm^{-1} Schiff base band in Figure 4A are assigned to the BSI intermediate.

In the BSI Raman spectrum (Figure 3E), the ethylenic mode is a strong band at 1552 cm^{-1}, which is consistent with the correlation of the ethylenic frequencies of retinals with their absorption maxima.[35,36] In the fingerprint region, five bands at 1159, 1196, 1212, 1245, and 1278 cm^{-1} are observed. Interestingly, the fingerprint vibrational pattern of BSI is identical with that of Batho[9] as well as that of the *all-trans* retinal protonated Schiff base (PSB).[37] By analogy to the vibrational assignment work on Batho and the *all-trans* PSB, the band at 1159 cm^{-1} in BSI is assigned to the C_{10}-C_{11} stretch, which is the same as that of the *all-trans* PSB and ~7cm^{-1} below that of Batho. The 1196 cm^{-1} band is due to the C_{14}-C_{15} stretch, the 1212 cm^{-1} band is assigned to the C_8-C_9 stretch, and the 1246 cm^{-1} band is assigned to the C_{12}-C_{13} stretch. The band at 1278 cm^{-1} corresponds to the 11H + 12H rock.

BSI exhibits a new intense HOOP band at 886 cm^{-1} that was not observed in the Lumi and Meta I intermediates as well as two lines at 945 and 1009 cm^{-1}, which also appear in Lumi and Meta I.[20,38] The HOOP modes of the ethylenic protons across the 11d12 double bond of *all-trans* retinal derivatives form A_u and B_g local symmetry combinations found near 960 and 830 cm^{-1}, respectively, while the 10H and 14H wags are found around 880 cm^{-1}.[39,40] The 945 and 1009 cm^{-1} modes are assigned to the 11H and 12H A_u wag and methyl rocking vibration modes, respectively, based on frequency correspondence.[39,41] However, the frequency of the A_u HOOP mode in BSI is 6 cm^{-1} lower than that of Lumi and 12 cm^{-1} below that of Meta I. The unambiguous assignment of the 886 cm^{-1} band was accomplished by isotopic labeling. The 886 cm^{-1} mode is assigned as an isolated 14H wag, since it shifts to 737 cm^{-1} in 14d BSI (Figure 4A), with the expected H/d frequency ratio of 1.20.[8]

Figure 5 presents the transient Raman spectrum of BSI with a 250 ns time delay in d_2O buffer. The insert compares the Schiff base region of BSI in H_2O with that in D_2O. The 1653cm^{-1} Raman band in the Schiff base region of BSI in H_2O shifts to 1630 cm^{-1} after the protein is suspended in d_2O buffer. We conclude that the Schiff base group in BSI is protonated due to the coupling of the CdN stretch with the N-H rocking vibration. The Schiff base CdN mode at 1653 cm^{-1} in the BSI spectrum is similar to that of rhodopsin and Batho, but the d_2O-induced shift for BSI (~23 cm^{-1}) is smaller than that for rhodopsin and Batho. This shift is identical with that of Meta I as well as that of the M*all-trans* PSB. In Figure 5, we also note that the new HOOP band at 886 cm^{-1} shifts up 3 cm^{-1} in D_2O, whereas the frequencies of the HOOP modes

at 945 and 1009 cm^{-1} are unaffected by N-deuteriation. This sensitivity of the 886 cm^{-1} HOOP band shows that there is a coupling of this HOOP mode with 15 NH coordinate. A similar result was observed in *all-trans* bacteriorhodopsin, where the $C_{14}H$ wag frequency shifts from 882 cm^{-1} in H_2O to 886 cm^{-1} in D_2O.[42] This observation provides additional support for the C_{14}-H wag assignment.

Discussion

Time-resolved resonance Raman spectroscopy is valuable because it provides vibrational structural data on transient photoactive molecules in their native protein binding pocket environment.[43,44] Here we have performed time-resolved resonance Raman microchip flow experiments and obtained transient Raman spectra of the retinal chromophore in the BSI intermediate of rhodopsin. We will now compare these vibrational data with rhodopsin's other intermediates such as Batho, Lumi, and Meta I to elucidate the chromophore structural changes and interactions with the protein during the transitions from Bathoto-BSI and BSI-to-Lumi.

Structure of BSI. Figure 6 presents a summary comparison of the resonance Raman spectra of rhodopsin and its photointermediates. Figure 7 presents a correlation diagram of the HOOP, fingerprint, ethylenic, and C=NH as well as C=Nd modes for rhodopsin's intermediates and the *all-trans* retinal protonated Schiff base (PSB). The resonance Raman spectrum of Batho exhibits unusually intense hydrogen out-of-plane wagging vibrations at 853, ~872, and 921 cm^{-1} that are not observed in the spectrum of rhodopsin, Lumi, and Meta I. In addition, the $C_{11}H$ and $C_{12}H$ wags in Batho are unusually decoupled. The isolated band at 921 cm^{-1} in Batho is assigned as the 11H wag, and the 12H wag is placed between 850 and ~870 cm^{-1}.[45] Local perturbation near C_{12}-H is postulated as the cause of the low intrinsic $C_{12}H$ wag frequency. The more normal coupled $C_{11}H$=$C_{12}H$ HOOP frequency at 945 cm^{-1} in BSI shows that the transition from Batho to BSI involves a relaxation of the chromophore from a strained *all-trans* conformation and the elimination of the structural perturbation that uncouples the 11H and 12H wags. The $C_{10}H$ wag intensity is significantly reduced in BSI, Lumi, and Meta I. This gives further evidence of a chromophore structural relaxation in the Batho-to-BSI transition. However, a relatively intense HOOP band at 886 cm^{-1} is observed in BSI, which is assigned to the $C_{14}H$ wag. The 853 cm^{-1} $C_{14}H$ wag is also quite intense in Batho,[8] but its intensity goes away in Lumi. Therefore, we conclude that the structure of BSI is still locally twisted near C_{14}.

The frequencies of the 11,12-A_u HOOP mode in BSI, Lumi, and Meta I are 19, 13, and 7 cm^{-1}, respectively, lower than that of *all-trans* retinal PSB (964 cm^{-1}). Thus, the coupling of the 11H and 12 H wags is significantly decreased in BSI but only somewhat decreased in Lumi and Meta I. This observationsupports the idea that Lumi has a more relaxed chromophore structure and that this relaxation is complete in Meta I.[20,27,46-48]The unusually low frequency of the 11,12 A_u HOOP mode and the weaker coupling of the $C_{11}H$ and $C_{12}H$ wags suggests that this region is significantly conformationally distorted in BSI,[49] but this perturbation is not as great as that found in Batho.

Comparison of the fingerprint modes also provides information on structural changes during the transition from Batho to BSI. The 1166 cm^{-1} C_{10}-$_{11}$ stretch of Batho is 7 cm^{-1} higher than that in the *all-trans* retinal PSB, while this mode drops 7 cm^{-1} to the PSB frequency in BSI. However, the C_{10}-C_{11}stretching modes of Lumi and Meta I are 4 and 6 cm^{-1}, respectively, lower than that of *all-trans* retinal PSB (Figure 7). This result suggests that the formation of BSI does not require a significant conformation distortion around the C_{10}-C_{11} bond, consistent with its weak $C_{10}H$ wag intensity. Similarly, the 1210 cm^{-1} C_{14}-C_{15} stretch of Batho is 6 cm^{-1} above its PSB value while in BSI it is 2 cm^{-1} above the PSB value. On the other hand,

the C_{12}-C_{13} and C_8-C_9 stretching modes are very similar to each other in Batho, BSI, Lumi, and Meta I.

Schiff Base Environment of BSI. The C=N stretching vibration of the Schiff base provides a sensitive probe of chromophore-protein interactions.[45,50,51] As summarized in Figure 7, the C=N stretching mode in BSI is observed at 1653 cm^{-1}, which is identical with that of rhodopsin and Batho. However, the shift induced by deuteriation is decreased from ~30 cm^{-1} in rhodopsin and Batho to 23 cm^{-1} in BSI. The reduced isotope shift indicates that the coupling of the C=N stretch with the N-H bending vibration in BSI is reduced somewhat, implying there is a modest change of the protonated Schiff base environment upon formation of BSI from Batho. However, there is no large protein relaxation in the Batho-to-BSI transition. Kinetic studies of the artificial pigment cis-5, 6-dihydroisorhodopsin[15] also suggested that the rate of the Batho-to-BSI transition is limited by the relaxation of the strained *all-trans* retinal chromophore within a tight protein environment. However, it is interesting that in Lumi the C=N stretching mode is unusually low compared to BSI and all the other intermediates; the weaker coupling of the C=N stretch with the N-H bending vibration leads to onlya7cm^{-1} D_2O induced shift. The dramatically weakened Schiff base hydrogen bonding, suggesting that there is essentially no H-bond acceptor in Lumi, recovers to the *all-trans* PSB value with the transition to Meta I.[20] The unusual Schiff base environment formed in Lumi demonstrates that the transition of BSI to Lumi involves a conformational change of the chromophore and the residues in the vicinity of the chromophore that dramatically alters the Schiff base hydrogen bonding. Consistent with this observation, kinetic absorption measurements[17] and FTIR data on artificial chromophore analogues[11,16] suggested that BSI formation does not involve large protein structural changes while the formation of Lumi is primarily determined by protein changes.

Protein Response. Since the protein provides a well-defined and specific “solvent cage” around the chromophore, the chromophore vibrational structure can be used as a probe of the protein binding pocket environment and its structural changes. The protein response to the 200 fs isomerization reaction in rhodopsin consists of first a local impulsive structural rearrangement that is driven by chromophore isomerization[6] followed by a diffusive motion that allows for more global energy redistribution within the chromophore-protein complex. Picosecond transient resonance Raman studies on photorhodopsin and bathorhodopsin suggested that a localized region of the highly specific protein binding pocket responds impulsively to ultrafast isomerization of the chromophore thereby permitting the isomerization reaction to occur efficiently in a tight and specific binding pocket in only 200 fs.[6] It is reasonable to expect that such an inertial protein response is localized primarily in the region near C_{11}=C_{12} where the largest chemical shift differences upon isomerization were observed.[52] However, other more delocalized protein degrees of freedom remain relatively static on the same time scale in order to efficiently store energy. For example, the C=N stretch frequencies and the Nd shifts of rhodopsin and Batho are identical, indicating that the interaction between the Schiff base and the Glu113 counterion environment remains unchanged during the transition from rhodopsin to Batho.

The transient BSI Raman data suggest that, except for the C_{14} region, the highly strained all-trans chromophore in Batho has relaxed. Additionally, a slight change of Schiff base environment appears in the Batho-to-BSI transition. This suggests that the delocalized protein response due to collective conformational motions[53] is slower than BSI formation. A large time-scale separation between chromophore and binding pocket motion has been suggested by time-resolved CARS studies,[54] because the Batho vibrational spectrum is unaltered out to 100 ns after Batho formation. Therefore, the BSI-to-Lumi transition is likely to be the stage where the stored photon energy is transferred from the strained chromophore to the more broadly distributed protein modes, producing a more relaxed Lumi intermediate as well as the driving force to move the Schiff base group out of its hydrogen-bonded environment near Glu113.

Conclusions

We have obtained time-resolved resonance Raman spectra of the native BSI intermediate of rhodopsin. By combining these data with time-resolved resonance Raman spectra of the other intermediates we can compare the vibrational structure changes for all of rhodopsin's photointermediates for the first time (Figures 6 and 7). Furthermore, a molecular model of the retinalbinding pocket for rhodopsin's intermediates is presented in Figure 8 to begin exploring how the chromophore structural changes interact with the protein. Batho, the first thermally relaxed intermediate after photoisomerization of rhodopsin, has a highly strained all-trans chromophore structure; the -20° twist angles at C_{10}-C_{11} and C_{12}-C_{13} and the -56° twist at C_{14}-$C_{15}$are consistent with the resonance enhancement of Batho HOOP modes. In the model, W265 moves toward C_{12} in the rhodopsin-Batho transition (5.5 → 4.7 Å), while E181 moves away from C_{12} (4.6 → 4.9 Å). W265 may thus be one of the residues responsible for the perturbation near C_{11}=C_{12} in Batho. Further, W265 is the closest residue to the C_{13}-methyl group (3.4 Å) in rhodopsin. This unique environment due to the proximity of W265 to the retinal chromophore implies that steric interaction between the C_{13}-methyl group and W265 could play an important role in driving the initial isomerization dynamics. Femtosecond absorption experiments show that removal of the 13-methyl group slows down the isomerization to 400 fs and lowers the quantum yield to 0.47.[55,56] Cis-trans isomerization also moves the C_{13}-methyl group closer to E181 in Batho (6.2 → 3.0 Å). However, experimentally the rhodopsin-to-Batho transition does not alter the Schiff base environment. Therefore, the structural water forming a hydrogen bond from the PSB to E113 is still present in Batho. The Batho-to-BSI transition leads to a relaxation of the chromophore from a strained all-trans conformation and the elimination of much of the structuralperturbation except for a twist near C_{14}. As a result, the distance between W265 and C_{12} increases only 0.1 Å in the transition of Batho to BSI, and the twist angle of C_{14}-C_{15} in BSI relaxes to -46° (Figure 8C). The BSI-to-Lumi transition involves formation of a more relaxed all-trans chromophore structure as well as significant protein alteration. In the model, water is no longer hydrogen bonded to the PSB causing the unusual Lumi Schiff base properties (Figure 8D). The change in the Schiff base environment in Lumi also causes its polyene chain to move away from helix VI, closer to helix III, thereby moving the C_{13}-methyl group closer to E181 (3.1 → 3.0 Å). We have suggested that this movement reverts in the formation of Meta I[20] and that a fully relaxed chromophore with a normal Schiff base environment but a different hydrogen-bond acceptor is formed.

Acknowledgment

This work was supported by a grant from the NIH (EY02051). We thank Michael J. Tauber, david McCamant, and Elsa Yan for technical assistance and helpful discussions, Elisa Lau for expert assistance with the rhodopsin preparations, and Joe Lo for making the microfabricated Raman flow chip.

References

(1). Mathies, RA.; Lugtenburg, J. Handbook of Biological Physics. In: Stavenga, DG.; deGrip, WJ.; Pugh, EN., Jr., editors. Vol. 3. Elsevier Science Press; Amsterdam, The Netherlands: 2000. p. 55-90.

(2). Schoenlein RW, Peteanu LA, Mathies RA, Shank CV. Science 1991;254:412–415. [PubMed: 1925597]

(3). Peteanu LA, Schoenlein RW, Wang Q, Mathies RA, Shank CV. Proc. Natl. Acad. Sci. U.S.A 1993;90:11762–11766. [PubMed: 8265623]

(4). Kim JE, Tauber MJ, Mathies RA. Biochemistry 2001;40:13774–13778. [PubMed: 11705366]

(5). Kandori H, Shichida Y, Yoshizawa T. Biophys. J 1989;56:453–457. [PubMed: 2790133]

(6). Kim JE, McCamant DW, Zhu L. Mathies. R.A.J. Phys. Chem. B 2001;105:1240–1249.

(7). Stryer L. Annu. ReV. Neurosci 1986;9:87–119. [PubMed: 2423011]

(8). Eyring G, Curry B, Broek A, Lugtenburg J, Mathies R. Biochemistry 1982;21:384–393. [PubMed: 7074022]

(9). Palings I, Pardoen JA, van den Berg E, Winkel C, Lugtenburg J, Mathies RA. Biochemistry 1987;26:2544–2556. [PubMed: 3607032]

(10). Bagley KA, Balogh-Nair V, Croteau AA, Dollinger G, Ebrey TG, Eisenstein L, Hong MK, Nakanishi K, Vittitow J. Biochemistry 1985;24:6055–6071. [PubMed: 4084506]

(11). Ganter UM, Gartner W, Siebert F. Biochemistry 1988;27:7480–7488. [PubMed: 3207686]

(12). Birge RR. Biochim. Biophys. Acta 1990;1016:293–327. [PubMed: 2184895]

(13). Shieh T, Han M, Sakmar TP, Smith SO. J. Mol. Biol 1997;269:373–384. [PubMed: 9199406]

(14). Lewis JW, Szundi I, Fu W-Y, Sakmar TP, Kliger d. S. Biochemistry 2000;39:599–606. [PubMed: 10642185]

(15). Hug SJ, Lewis JW, Einterz CM, Thorgeirsson TE, Kliger DS. Biochemistry 1990;29:1475–1485. [PubMed: 2334708]

(16). Ganter UM, Kashima T, Sheves M, Siebert F. J. Am. Chem. Soc 1991;113:4087–4092.

(17). Randall CE, Lewis JW, Hug JW, Bjoörling SC, Eisner-Shanas I, Friedman N, Ottolenghi M, Sheves M, Kliger DS. J. Am. Chem. Soc 1991;113:3473–3485.

(18). Lewis JW, Pinkas I, Sheves M, Ottolenghi M, Kliger DS. J. Am. Chem. Soc 1995;117:918–923.

(19). Jaöger S, Lewis JW, Zvyaga TA, Szundi I, Sakmar TP, Kliger DS. Proc. Natl. Acad. Sci. U.S.A 1997;94:8557–8562. [PubMed: 9238015]

(20). Pan D, Mathies RA. Biochemistry 2001;40:7929–7936. [PubMed: 11425321]

(21). Applebury ML, Zuckerman DM, Lamola AA, Jovin TM. Biochemistry 1974;13:3448–3458. [PubMed: 4846291]

(22). Woolley AT, Mathies RA. Proc. Natl. Acad. Sci. U.S.A 1994;91:11348–11352. [PubMed: 7972062]

(23). Simpson PC, Woolley AT, Mathies RA. J. Biomed. Microdevices 1998;1:7–26.

(24). Mathies R, Oseroff AR, Stryer L. Proc. Natl. Acad. Sci. U.S.A 1976;73:1–5. [PubMed: 1061102]

(25). Mathies R, Yu N-T. J. Raman Spectrosc 1978;7:349.

(26). Palczewski K, Kumasaka T, Hori T, Behnke CA, Motoshima H, Fox BA, Le Trong I, Teller DC, Okada T, Stenkamp RE, Yamamoto M, Miyano M. Science 2000;289:739–745. [PubMed: 10926528]

(27). Verdegem PJE, Bovee-Geurts PHM, de Grip WJ, Lugtenburg J, de Groot HJM. Biochemistry 1999;38:11316–11324. [PubMed: 10471281]

(28). Creemers AFL, Klaassen CHW, Bovee-Geurts PHM, Kelle R, Kragi U, Raap J, de Grip WJ, Lugtenburg J, de Groot HJM. Biochemistry 1999;38:7195–7199. [PubMed: 10353830]

(29). Tan Q, Lou J, Borhan B, Karnaukhova E, Berova N, Nakanishi K. Angew. Chem., Int. Ed. Engl 1997;36:2089–2093.

(30). Lou J, Hashimoto M, Berova N, Nakanishi K. Org. Lett 1999;1:51–54. [PubMed: 10822532]

(31). Buss V, Kolster K, Terstegen F, Varenhorst R. Angew. Chem., Int. Ed. Engl 1998;37:1893–1895.

(32). Eyring G, Curry B, Mathies R, Fransen R, Palings I, Lugtenburg J. Biochemistry 1980;19:2410–2418. [PubMed: 7387982]

(33). Verhoeven MA, Creemers AFL, Bovee-Geurts PHM, de Grip WJ, Lugtenburg J, de Groot HJM. Biochemistry 2001;40:3282–3288. [PubMed: 11258947]

(34). Eilers M, Reeves PJ, Ying WW, Khorana HG, Smith SO. Proc. Natl. Acad. Sci. U.S.A 1999;96:487–492. [PubMed: 9892660]

(35). Kochendoerfer GG, Wang Z, Oprian DD, Mathies RA. Biochemistry 1997;36:6577–6587. [PubMed: 9184137]

(36). Albeck A, Livnah N, Gottlieb H, Sheves M. J. Am. Chem. Soc 1992;114:2400–2411.

(37). Smith SO, Myers AB, Mathies RA, Pardoen JA, Winkel C, van den Berg EMM, Lugtenburg J. Biophys. J 1985;47:653–664. [PubMed: 4016185]

(38). Ohkita YJ, Sasaki J, Maeda A, Yoshizawa T, Groesbeek M, Verdegem PJE, Lugtenburg J. Biophys. Chem 1995;56:71–78. [PubMed: 7662871]

(39). Curry B, Broek A, Lugtenburg J, Mathies R. J. Am. Chem. Soc 1982;104:5274–5286.

(40). Curry B, Palings I, Broek A, Pardoen JA, Mulder PPJ, Lugtenburg J, Mathies R. J. Phys. Chem 1984;88:688–702.

(41). Smith SO, Braiman MS, Myers AB, Pardoen JA, Courtin JML, Winkel C, Lugtenburg J, Mathies RA. J. Am. Chem. Soc 1987;109:3108–3125.

(42). Smith SO, Myers AB, Pardoen JA, Winkel C, Mulder PPJ, Lugtenburg J, Mathies R. Proc. Natl. Acad. Sci. U.S.A 1984;81:2055–2059. [PubMed: 16593445]

(43). Mathies, RA.; Smith, SO.; Palings, I. Biological Applications of Raman Spectroscopy: Resonance Raman Spectra of Polyenes and Aromatics. In: Spiro, TG., editor. Vol. 2. John Wiley and Sons; New York: p. 59-108.

(44). van den Berg R, Jang d. J. Bitting HC, El-Sayed MA. Biophys. J 1990;58:135–141.

(45). Palings I, van den Berg EMM, Lugtenburg J, Mathies RA. Biochemistry 1989;28:1498–1507. [PubMed: 2719913]

(46). doukas AG, Aton B, Callender RH, Ebrey TG. Biochemistry 1978;17:2430–2435. [PubMed: 678522]

(47). Siebert F. Isr. J. Chem 1995;35:309–323.

(48). Kliger, d. S.; Lewis, JW. Isr. J. Chem 1995;35:289–307.

(49). Tasumi, M. IUPAC International Congress on Analytical Sciences 2001. In: Sawada, T., editor. The Japan Society for Analytical Chemistry; Waseda Univeristy, Tokyo: p. 148

(50). deng H, Callender RH. Biochemistry 1987;26:7418–7426. [PubMed: 3427083]

(51). Baasov T, Friedman N, Sheves M. Biochemistry 1987;26:3210–3217. [PubMed: 3607019]

(52). Smith SO, Courtin J, de Groot HJM, Gebhard R, Lugtenburg J. Biochemistry 1991;30:7409–7415. [PubMed: 1649627]

(53). Riter RR, Edington M. d. Beck WF. J. Phys. Chem 1996;100:14198–14205.

(54). Jaöger F, Ujj L, Atkinson GH. J. Am. Chem. Soc 1997;119:12610–12618.

(55). Wang Q, Kochendoerfer GG, Schoenlein RW, Verdegem PJE, Lugtenburg J, Mathies RA, Shank CV. J. Phys. Chem 1996;100:17388–17394.

(56). Kochendoerfer GG, Verdegem PJE, van der Hoef I, Lugtenburg J, Mathies RA. Biochemistry 1996;35:16230–16240. [PubMed: 8973196]

Figure 1.
Time-resolved resonance Raman microchip flow apparatus. The two cylindrically focused laser beams (3 × 100 μm) are displaced along the flow direction to establish the time resolution. To obtain a resonance Raman spectrum of BSI, the two laser beams were separated by ~0.7 μm and a flow rate of 280 cm/s gave a pump-probe time delay of ~ 250 ns. The expanded chip view shows just the bottom etched wafer that makes up the bonded 2-layer glass sandwich structure. The beam paths indicated are not drawn to scale.

Figure 2.

Temporal evolution of the relative concentrations of Rho, Batho, BSI, and Lumi, where $k_1^f = k_1^r = 4.44 \times 10^6\ s^{-1}$, $k^2 = 3.4 \times 10^6\ s^{-1}$, and $k_3 = 1.0 \times 10^5\ s^{-1}$ at 5 °C (ref 15). The photoisomerization rate was given by $k = 1.31 \times 10^5 \exp(-6.6t^2)$, which describes the time-dependent photoisomerization of rhodopsin in a volume element of the sample as it passes through the Gaussian profile laser beam (ref 24). The 531 nm light intensity at the 3 × 100 μm beam waist is 2.2×10^{21} photons $cm^{-2}\ s^{-1}$. The flow rate and transit time are 280 cm/s and 1.1 μs, respectively.

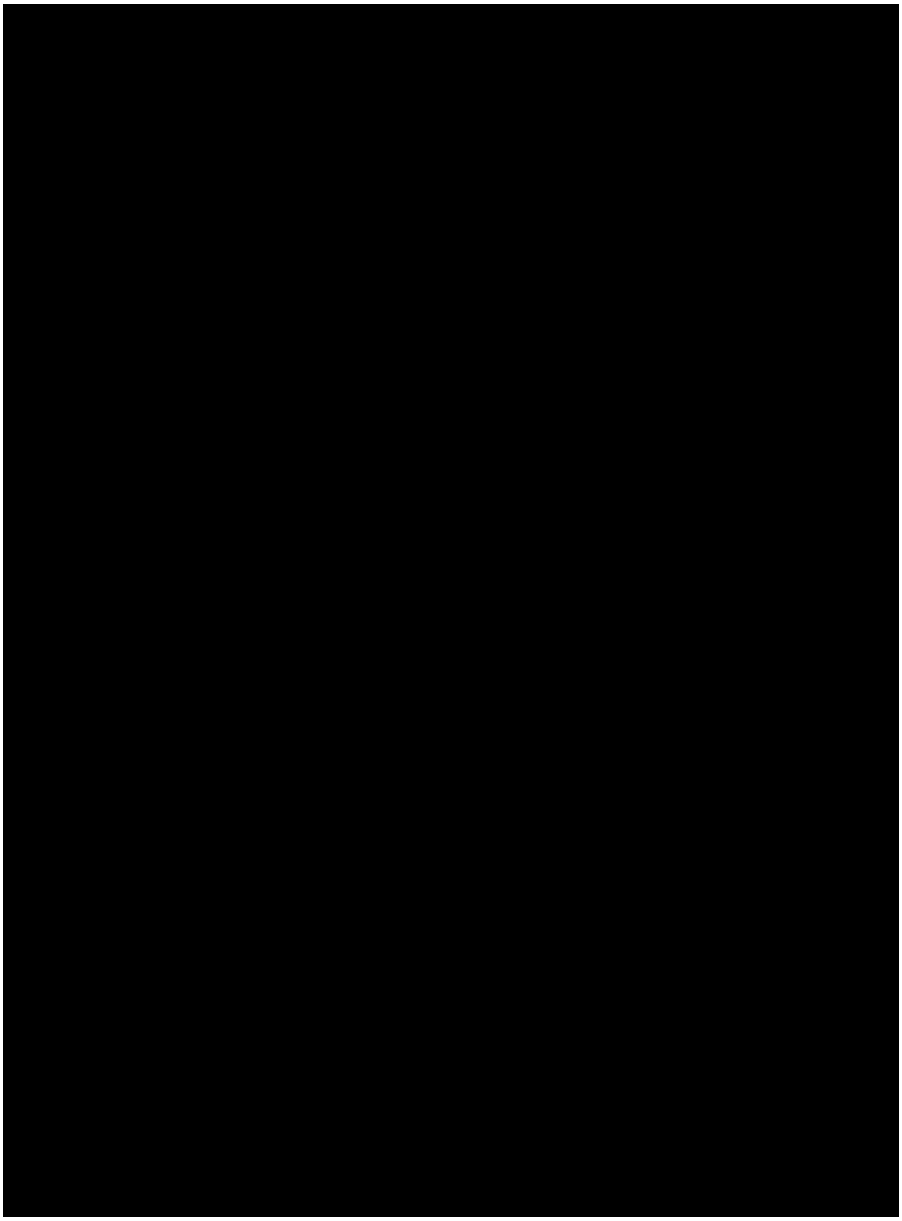

Figure 3.

Raman microchip flow spectra of rhodopsin's BSI intermediate: (A) pump-plus-probe spectrum, (B) probe-only spectrum, (C) transient spectrum obtained by subtracting 86% of the probe-only spectrum from the pump-plus-probe spectrum, (D) the Lumi spectrum with a 3 μs time delay, and (E) the BSI spectrum obtained by subtracting the indicated fraction of the Lumi spectrum from the transient spectrum. The optimum subtraction coefficient was determined to be 0.5 ± 8%. The pump wavelength was 531 nm (2.5 mW) and the probe was 458 nm (450 μW). The 250 ns time delay was provided by a 280 cm/s flow rate and the 0.7 μm displacement between the 3 × 100 μm pump and probe beams.

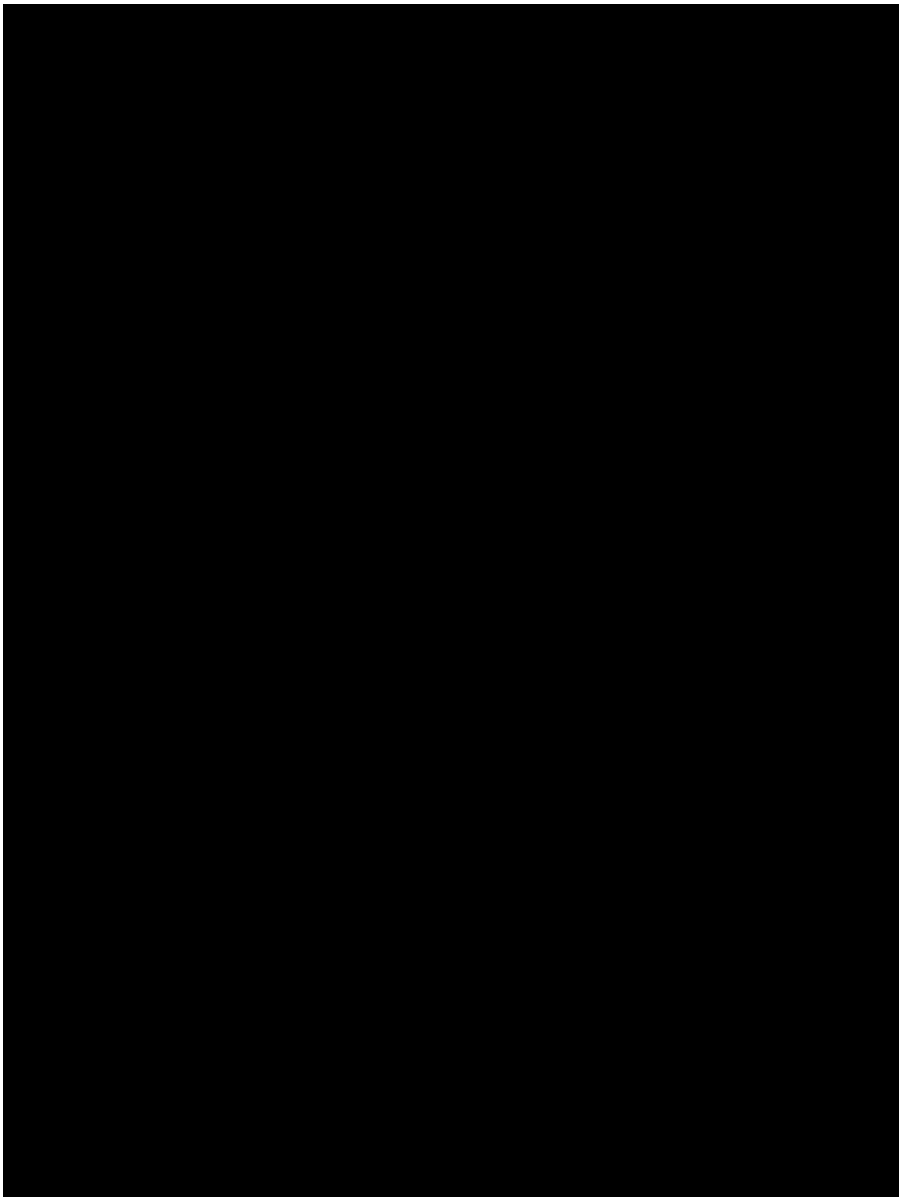

Figure 4.

Kinetic Raman spectra of the BSI and Lumi intermediates at the indicated time delays (7 °C). All spectra were obtained by subtracting the optimized fraction of the probe-only spectrum from the corresponding pump-plus-probe spectrum. The insert in spectrum A presents the 600-900 cm^{-1} region of the Raman spectrum of the 14D derivative of BSI at 250 ns time delay. The 700 ns time delay was provided by a separation of 2 μm and a flow speed of 260 cm/s. The 3 μs time delay was provided by a separation of 8 μm and a 250 cm/s flow speed. The pump and probe excitation wavelengths were 531 and 458 nm, respectively.

Figure 5.
Transient resonance Raman spectrum of BSI with a 250 ns time delay in D_2O buffer. The insert compares the Schiff base region of the Raman spectra of BSI in H_2O and D_2O.

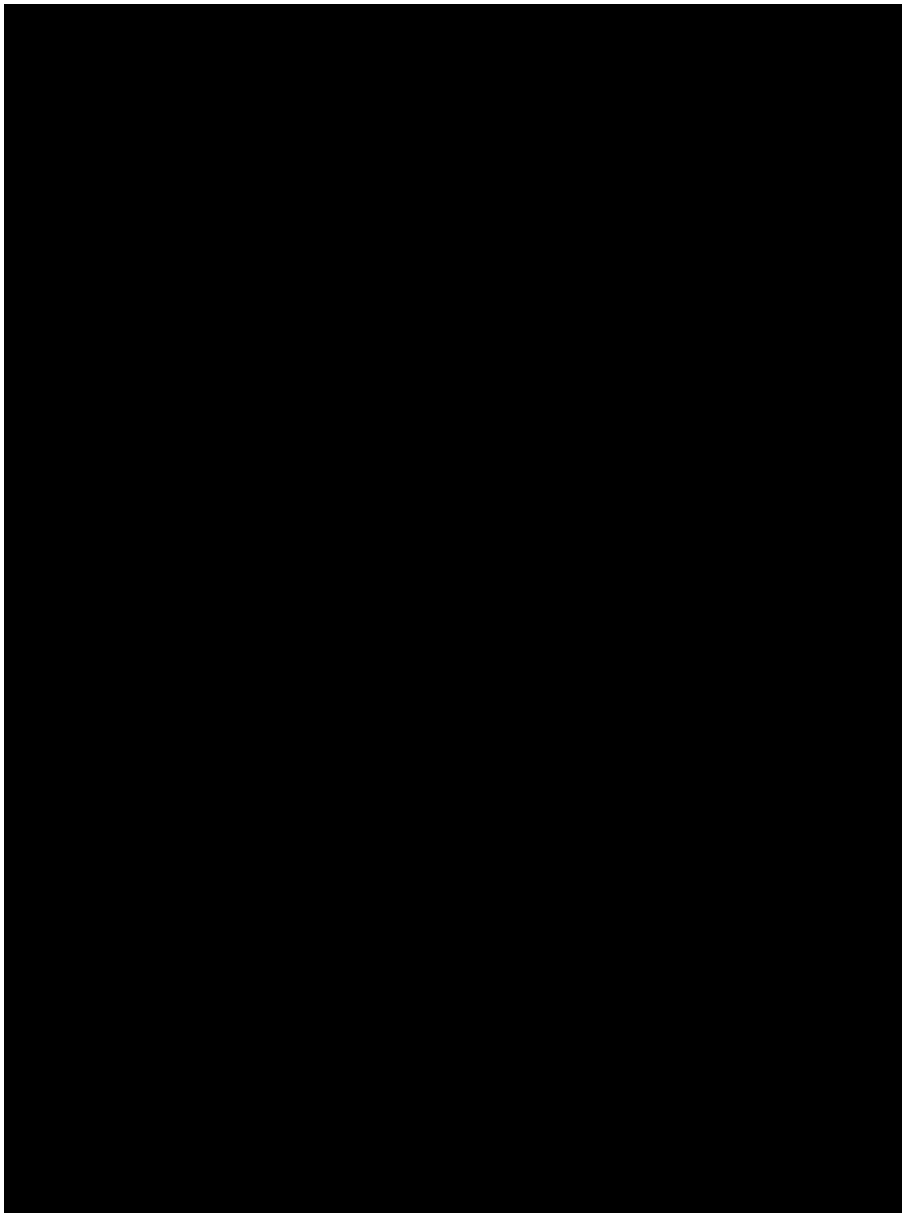

Figure 6.
Room-temperature time-resolved resonance Raman spectra of rhodopsin and its intermediates. The rhodopsin spectrum was obtained with 458 nm excitation. The Batho spectrum with 20 ps time delay at room temperature is reproduced with permision from Kim et al. (ref 6). The Lumi and Meta I spectra are from our previous study (ref 20).

Figure 7.
Correlation diagram of the HOOP, fingerprint, ethylenic, and Schiff base mode frequencies observed in rhodopsin, bathorhodopsin, lumirhodopsin, metarhodopsin I, and the *all-trans* retinal protonated Schiff base (PSB). The frequencies of the *all-trans* PSB were obtained from spectra in methanol solution (ref 37), which provide a common reference for the protein binding pocket induced effect.

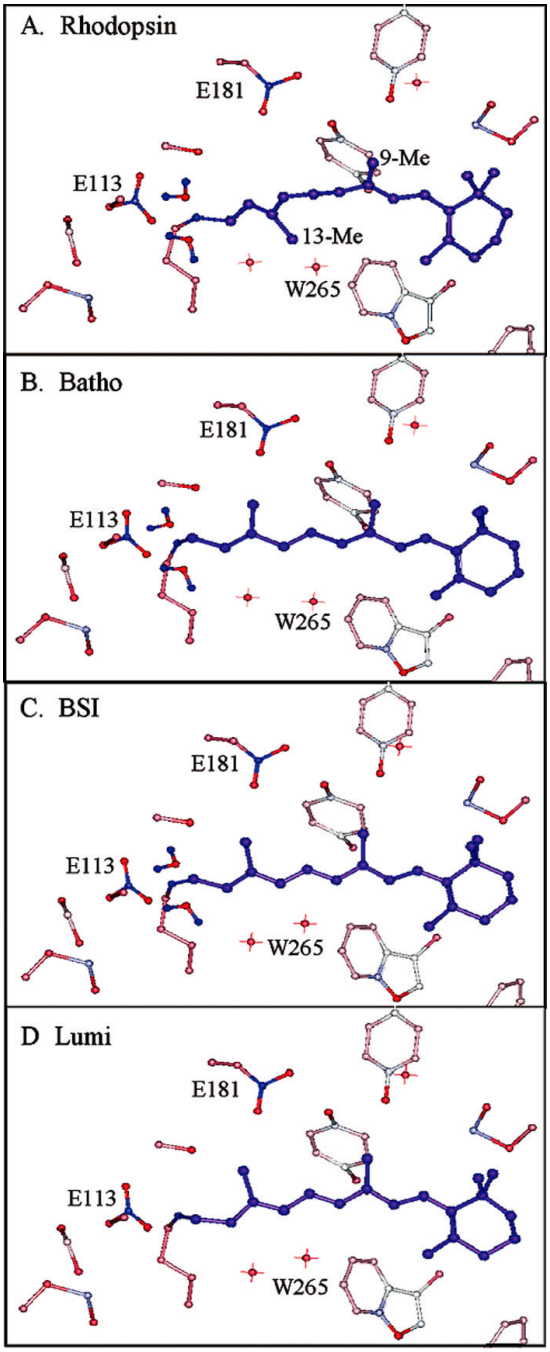

Figure 8.

Graphics model of the retinal binding site in rhodopsin illustrating the structural changes in the primary photoactivation. (A) The 11-*cis*rhodopsin structure: The C_{12}-C_{13} twist angle of -140° dictates that the 13-Me group extends out of the page. The distance of the PSB proton to the carbon atom of E113 is 4.3 Å (ref 28). (B) Batho structure: The twist angles of C_{10}-$C_{11}$and C_{12}-C_{13} are -20°, and the twist angle of C_{14}-$C_{15}$is -56°. The carbon atom of E113 is located 4.3 Å away from the PSB proton. (C) BSI structure: The twist angles of C_{10}-C_{11}, C_{12}-$C_{13,}$ and C_{14}-C_{15} are -9°, -10°, and -46°, respectively. (D) Lumi structure: The twist angles of C_{10}-C_{11}, C_{12}-C_{13}, and C_{14}-C_{15} are -4°, -2°, and -9°, respectively. The distances of the PSB proton to the carbon atom of E113 in BSI and Lumi are 3.8 and 4.0 Å, respectively.